

1

INTRODUCTION

Since the first detection of exoplanet 51 Pegasi b, the discoveries have been boosted significantly. Till now, about 6,000 exoplanets have been found (Fig. 1.1), but Earth remains the only known planet that hosts life. This contrast forces upon us fundamental questions: Are we really alone in the Universe? What is the origin of life?

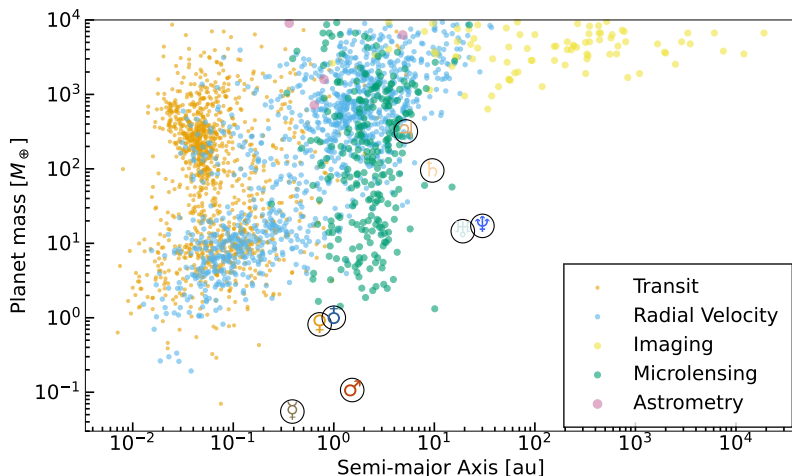


Figure 1.1. Planet mass versus semi-major axis for all confirmed exoplanets (NASA Exoplanet Archive, retrieved January 2026). Exoplanets are color- and size-coded by discovery method. The Solar System planets are indicated with their astronomical symbols.

However, our view of the exoplanet population is intrinsically incomplete and distorted. The observations are biased in different ways, depending on which exoplanet detection method is used. **Transit Photometry** detects the eclipsing behavior of a planet passing in front of its host star. It is heavily biased toward planets on short-period orbits, as they transit more frequently and have a higher geometric probability of alignment with our line of sight. **Radial Velocity** measures the star's Doppler shift in its light caused by the gravitational pull of an orbiting planet. It is most sensitive to massive planets in moderately close orbits, as these induce a larger and more rapid stellar motion. **Direct Imaging** directly captures light from the planet itself. It is biased toward massive, young planets on very wide orbits.

Young planets are sufficiently hot (after accretion) and bright, and the wide separations help to avoid stellar glare. **Astrometry** tracks the star's spatial shift on the sky due to the orbital motion of massive companions. It is most effective for massive planets at intermediate orbital distances, where the stellar wobble is both significant and occurs over an observable timescale. **Microlensing** can detect foreground planets due to their gravitational lensing effect, which magnifies the light of a background star when temporarily passing through it. It probes planets, including cold super-Earths, at orbital distances typically near or beyond 1 AU. But the detailed orbital characterization remains challenging in this way.

Therefore, current observations alone cannot determine whether Earth is intrinsically rare or common. While the construction of larger, more sensitive telescopes represents the definitive long-term path forward, the essential near-term work lies in understanding planet formation processes as much as possible based on the present observational abilities.

1.1 Planet formation

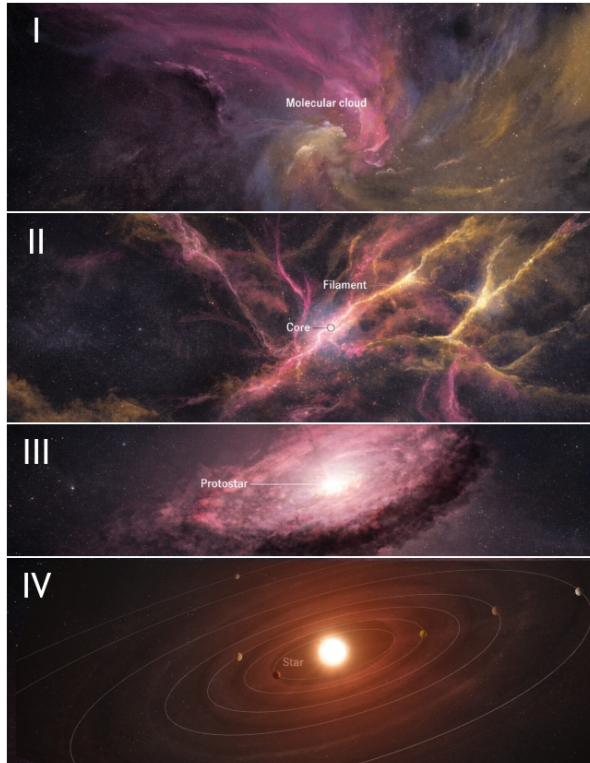


Figure 1.2. Simple illustration of star formation stages. Stage I, molecular cloud. Stage II, stars form during core collapse. Stage III, circumstellar disk around a protostar. Stage IV, mature planet system. Credit: Matthew Twombly (Panel I, II, III) and NASA/Daniel Rutter (Panel IV)

The formation of a planet system begins with the gravitational collapse of a cold, dense region within a giant molecular cloud. As shown in Fig. 1.2, this collapse fragments the cloud, with the most massive central core accreting the bulk of the material to form a protostar.

Some smaller fragments may directly collapse into isolated planetary-mass objects, denoting an early, direct formation pathway. Once the central protostar has obtained sufficient mass, its thermodynamic feedback halts further large-scale infall (Jeans 1902). Then, conservation of angular momentum forces the remaining material into a flattened, rotating protoplanetary disk. This disk is the perfect birthplace for planets. The Solar System also had such a disk 4.5 Gyr ago, often called the Solar Nebula.

1.1.1 Protoplanet disk

Protoplanetary disks are mostly composed of gas, initially 10% of the host mass, with about 1% solids. As the disk cools down, the local gravity becomes important and planets can form. This process is called Gravitational Instability. Similar to star formation, but the fragment of the protoplanet disk needs to balance Keplerian shearing additionally (Toomre 1964). GI might be happening violently in some disks like AB Aurigae (Speedie et al. 2024; Calcino et al. 2025).

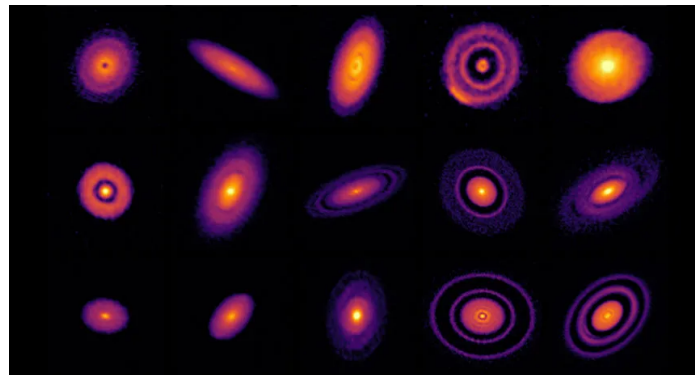


Figure 1.3. Continuum gallery of Dsharp disks imaged by ALMA (Andrews et al. 2018).

Planets also form through the alternative, bottom-up pathway of core accretion. Within the disk, microscopic dust grains collide and coalesce, gradually building larger bodies from planetesimals to planetary embryos. Embryos as small as the Moon can efficiently accrete pebbles (Ormel & Klahr 2010; Lambrechts & Johansen 2012), while closer to the star (within ~ 1 au), shorter collisional timescales allow for the accretion of numerous kilometre-sized planetesimals (Kokubo & Ida 1998). Upon reaching a critical mass of ~ 10 Earth masses, an embryo begins to accrete a gaseous envelope. When this envelope mass rivals the solid core mass, runaway gas accretion is triggered (Pollack et al. 1996), rapidly forming a gas giant. Concurrently, stellar radiation (Owen et al. 2012), disk viscosity (Shakura & Sunyaev 1976), and winds (Bai & Stone 2013) dissipate the remaining gas over several million years, leaving behind a mature planetary system whose architecture is dictated by the disk's initial temperature, density, and chemical gradients.

The advent of advanced facilities like ALMA, the VLT, and JWST now allows us to directly image protoplanetary disks in our galactic neighbourhood. Millimeter-wavelength observations, such as those from the DSHARP survey shown in Fig. 1.3, reveal that disks are not smooth; they are richly structured with rings and gaps. The most compelling interpretation for these substructures is the presence of embedded, accreting protoplanets. However, alternative explanations like pressure bumps exist, highlighting the need for multi-wavelength

observations to confirm the planet candidates.

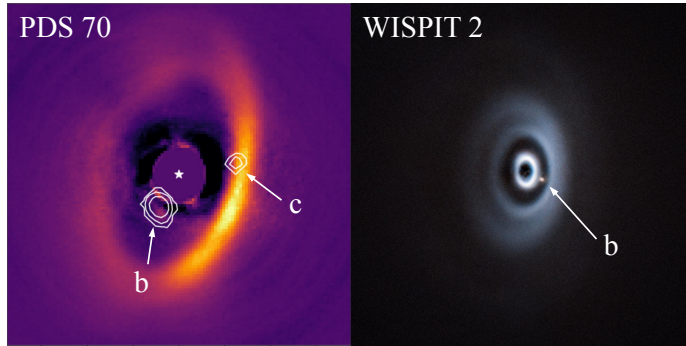


Figure 1.4. Protoplanets in PDS 70 (Haffert et al. 2019) and WISEA 2 (van Capelleveen et al. 2025). The disk data are collected via VLT/SPHERE.

To date, dozens of candidate protoplanets have been identified, with confirmed detections in two young, solar-type systems, as shown in Fig. 1.4. The protoplanets PDS 70 b and c and WISEA 2 b are located at substantial distances of approximately 20, 30, and 50 AU from their host stars, respectively. In both systems, the planets are confirmed because they are actively accreting surrounding disk material, a process so vigorous that it generates detectable H α emission induced by accretion shocks. In both systems, the protoplanets are gas giants. Their strong gravity clears the disk at their orbits and opens deep gaps.

1.1.2 Planet migration

Planets do not remain at their birth locations. While embedded in a gaseous protoplanetary disk, gravitational interactions between a planet and the surrounding gas exchange angular momentum, causing the planetary orbit to evolve — a process known as planet migration. This mechanism fundamentally shapes the final architecture of planetary systems and provides a natural explanation for close-in exoplanets observed today.

Depending on the planet’s mass and local disk conditions, migration proceeds in distinct dynamical regimes. Low-mass planets that do not strongly perturb the gas structure undergo Type I migration, a linear regime in which the migration rate scales with both the disk surface density and the planet’s mass. As planets grow and become gas giants, they carve deep, cleared gaps in the disk, transitioning into Type II migration. In this regime, migration is significantly slower because the flow of disk material across the gap is suppressed by the strong planet gravity (Kanagawa et al. 2017). In the following sections, I outline the primary physical torques responsible for this angular momentum exchange.

Lindblad Torque

The dominant contribution to planet migration arises from spiral density waves launched by the planet at Lindblad resonances in the disk. These resonances occur where the gas orbital frequency satisfies a simple commensurability with the planet’s orbital frequency (e.g. Lin & Papaloizou 1979). At these locations, the planet excites trailing spiral waves that propagate radially, exchanging angular momentum.

The torque exerted by the disk can be decomposed into contributions from the inner and outer disk. The inner disk typically exerts a positive torque on the planet, while the outer disk exerts a negative torque. In most disk models, the outer torque dominates, resulting in a net

negative torque known as the differential Lindblad torque. The magnitude and direction of the Lindblad torque depend primarily on the disk surface density and temperature gradients, as well as the planet's mass and the disk scale height. In locally isothermal disks, the Lindblad torque is almost always negative, leading to inward migration.

Corotation Torque

In addition to Lindblad torques, planets exchange angular momentum with gas in their co-orbital region, near the planet's orbital radius. Gas in this region executes horseshoe-shaped trajectories corotating with the planet. The leading horseshoe gives angular momentum to the planets, while the trailing horseshoe takes away angular momentum. The resulting net corotation torque can either slow down, halt, or even reverse migration depending on the gradients of vortensity (vorticity divided by surface density) and entropy across the horseshoe region (Paardekooper & Papaloizou 2009; Paardekooper et al. 2010).

However, the corotation torque is prone to saturation. In low-viscosity or weakly diffusive disks, the horseshoe region becomes phase-mixed, erasing the gradients that sustain the torque. Viscosity and thermal diffusion are therefore essential to maintain an unsaturated corotation torque.

New Torques and the disk inner edge

Beyond the classical Lindblad and corotation torques, recent theoretical and numerical work has identified additional torque components that can significantly alter migration behaviour.

One is the heating torque. Actively accreting planets release gravitational energy as localized heating, which modifies the gas density asymmetrically around the planet and produces an additional positive torque. This can slow or even reverse inward migration for low-mass, rapidly accreting planets (Benítez-Llambay et al. 2015; Masset 2017), and is especially relevant during early growth phases.

A recent study by Chrenko et al. (2024) has also shown that the process of pebble accretion can produce a significant outward torque on a planet, known as the pebble torque. As a planet accretes drifting pebbles, it creates an imbalance in the pebble distribution around its orbit. This asymmetry gives the planet angular momentum and can often reverse the typical inward migration driven by the gas disk, depending on the disk mass, pebble sizes, and planet mass.

The inner edge of the protoplanetary disk, where gas density drops abruptly, can act as a migration trap for low-mass planets. This halt occurs because the sharp density gradient at the edge generates an almost one-sided, strong, positive corotation torque, which can balance the outer one-sided negative Lindblad torque (Liu et al. 2017). In contrast, gap-opening gas giants are largely decoupled from the local disk structure. Their deep gaps reduce gas–planet interaction, allowing them to cross the inner edge and migrate into the cavity region (Ataiee & Kley 2021).

1.2 Mean motion resonance

The study of mean motion resonance (MMR) originated with the work of Pierre-Simon Laplace, who first explained the resonant orbital architecture of Jupiter's Galilean moons. Celestial mechanics has since formalized the dynamics of orbital resonance Murray & Dermott (1999). In recent decades, the discovery of numerous resonant exoplanet systems and the detection of resonant substructures in protoplanetary disks have placed MMRs within the modern context of planet formation.

Planet migration naturally leads to mean motion resonances. When planets undergo convergent migration, where the outer planet migrates inward faster than the inner planet,

they are driven toward orbital commensurabilities (or integer period ratios). If the mutual migration is sufficiently slow and eccentricity damping is moderate, the planets can be gravitationally captured into a resonance. The specific resonance attained depends on the migration rate, eccentricity damping timescales, and planet masses.

The left panel of Fig. 1.5 uses three N-body simulations to show how different migration speeds lead to capture into different resonances. Faster migration typically produces more compact orbital resonances. If a pair of planets is in a $p:q$ mean motion resonance, their orbital period ratio must satisfy

$$\frac{P_2}{P_1} \approx \frac{p}{q}, \quad (1.1)$$

where p and q are small integers, and subscripts 1 and 2 denote the inner and outer planets, respectively. Equivalently, the mean motions $n_i = 2\pi/P_i$ satisfy

$$pn_2 - qn_1 \approx 0. \quad (1.2)$$

In such configurations, gravitational perturbations accumulate coherently over many orbital periods.

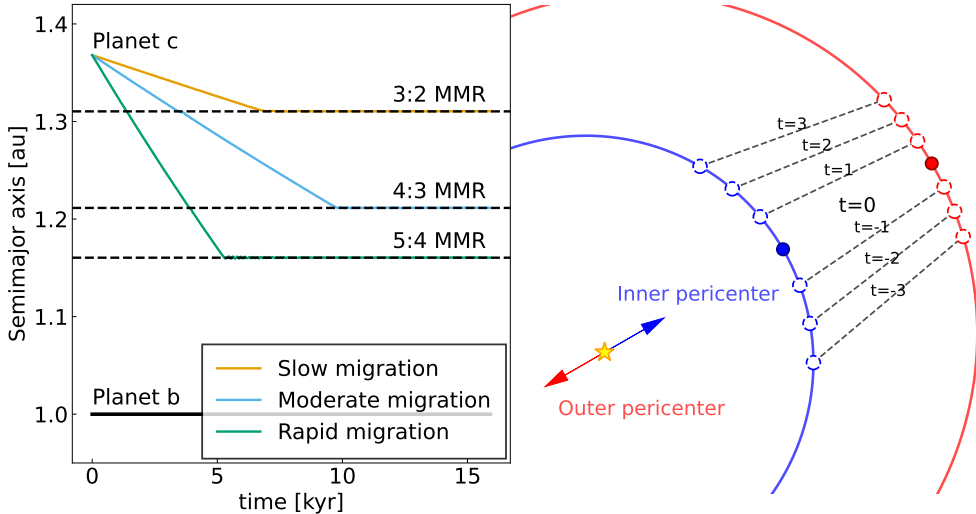


Figure 1.5. Left panel: Three restricted N-body simulations of resonant trapping for a low-mass planet c migrating inward toward a massive perturber b . Colored tracks show the orbital evolution of planet c under different migration timescales. Dashed vertical lines mark the nominal locations of mean-motion resonances with planet b . In this setup, planet b is treated as a fixed, massive central body whose orbit is not perturbed by planet c . Right panel: Schematic geometry of two planets locked in a mean-motion resonance. Planet conjunctions occur at a fixed phase, typically either aligned near the pericenter of the inner planet’s orbit or the apocenter of the outer planet’s orbit. This phase-locking enables stable, long-term angular momentum exchange that maintains the resonant configuration.

The defining feature of a mean motion resonance is the libration of one or more resonant angles. For a first-order resonance ($p:p-1$), a commonly used resonant angle is

$$\phi = p\lambda_2 - (p-1)\lambda_1 - \varpi_{1/2} = p(\lambda_2 - \varpi_{1/2}) - (p-1)(\lambda_1 - \varpi_{1/2}), \quad (1.3)$$

where $\lambda = M + \varpi$ is the mean longitude, M is the mean anomaly, and ϖ is the longitude of pericenter. Additional resonant angles involving ϖ_2 may also librate, depending on the system parameters.

The geometric interpretation of liberating resonance angles is that the conjunction longitude is fixed with respect to the planetary pericenters. As shown in Fig. 1.5 right panel, close encounters between the planets occur repeatedly at nearly the same orbital phase, typically near the pericenter (of the inner orbit) or the apocenter (of the outer orbit). If the encounter point is slightly off the pericenter or apocenter, the asymmetric torque between the planets will shift the next conjunction backwards. This phase-locking allows angular momentum exchange to occur coherently, maintaining the commensurability between the orbital periods while preventing close encounters.

Planets locked in such a resonant configuration are significantly more stable than non-resonant planets (circulating resonance angles) with integer period ratios (Hu et al. 2025b). Resonance capture thus represents a fundamental mechanism for sculpting stable, long-lived planetary architectures.

Three-Body Resonance

In systems containing three or more planets, resonant interactions can involve all planets simultaneously. A three-body mean motion resonance occurs when the orbital periods of three planets satisfy a single commensurability relation. A classic example is again the Laplace resonance among Jupiter's moons Io, Europa, and Ganymede, which satisfies

$$n_1 - 3n_2 + 2n_3 \approx 0, \quad (1.4)$$

where $n_i = 2\pi/P_i$ is the mean motion of the i -th planet.

Three-body resonances are characterized by the libration of a three-body resonant angle. Taking an example of zero-order three-body resonance, the form of the angle is

$$\phi_{3b} = -p\lambda_1 + q\lambda_2 - r\lambda_3 = q(\lambda_2 - \lambda_1) - r(\lambda_3 - \lambda_1), \quad (1.5)$$

where p , q , and r are integers satisfying $p - q + r = 0$. This angle can be derived from two body resonance angles by simply eliminating the pericenter term. If each adjacent pair of planets in a triplet is in resonance (with liberating two-body resonance angles), the three planets are by definition in three-body resonance. Unlike two-body resonances, these angles do not explicitly involve the longitudes of pericenter and can remain dynamically important even for nearly circular orbits.

However, three-body resonance is not simply the addition of two two-body MMRs. But the physical picture of three-body resonance can be understood as two-body resonance in a corotating frame of the innermost planet (Petit et al. 2020). Three-body resonances can also arise naturally during convergent migration, particularly in compact multi-planet systems where planets are sequentially captured into two-body resonances, forming resonant chains. But in some cases, individual two-body resonances may be disrupted while the three-body resonance persists, continuing to provide long-term dynamical protection and stability following a track in period ratio space (Papaloizou et al. 2018; Charalambous et al. 2018):

$$p \frac{P_2}{P_1} + r \frac{P_2}{P_3} = q, \quad (1.6)$$

and it is the time derivative of the mean-motion condition Eq. (1.4).

1.3 Planet architecture

1.3.1 Exoplanet systems

The dynamical complexity of a planetary system generally increases with the number of planets it contains. Multi-planet systems offer a rich laboratory to study planet formation and orbital evolution. Because as one more planet is introduced,

The architecture of exoplanet systems is very diverse. There are some planet systems in resonance: TRAPPIST-1, TOI-178, HR8799, PDS 70, etc. Most other planet systems do not exhibit resonance chains.

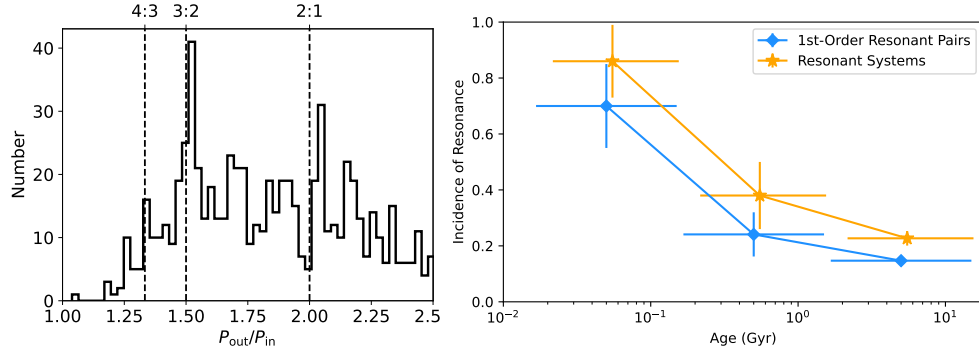


Figure 1.6. Left panel: Period ratio distribution of transiting exoplanets. Vertical dashed lines denote the resonant period ratios. Right panel: The fraction of planetary systems with at least one resonant pair (1st-order resonance in blue and 2nd-order resonance in orange) across three age bins. Figure adopted from Dai et al. (2024).

Fig. 1.6 (left panel) shows the period ratio distribution of transiting exoplanets. While most planet pairs lie just outside exact resonances, the presence of peaks near commensurate period ratios indicates that a certain fraction ($\approx 10\%$) of planets are captured into or have passed through mean motion resonances. These statistics have sparked considerable debate about the dominant pathways of planet formation:

1. The first school of thought argues that planets underwent substantial gas-driven migration and were initially trapped in resonance, but that roughly 80% of these chains later destabilized, potentially during the dispersal of the gaseous disk (Izidoro et al. 2017, 2021). Recent works further suggest that secular perturbations from an outer Earth-sized embryo (Ogihara & Kunitomo 2026), high-order resonance in the chain (Li et al. 2024), and planetesimal flybys (Li et al. 2025) can break an inner resonant chain.
2. A second view holds that many planets formed in gas-poor disks, where migration was inefficient (Ogihara et al. 2018; Choksi & Chiang 2020). In this scenario, large-scale resonant capture and the subsequent violent breaking of chains are largely absent.
3. A third perspective proposes that planets largely formed *in situ* after gas-disk dissipation. Clement et al. (2025) showed that terrestrial planet systems assembled in debris disks can reproduce the observed exoplanet statistics around M-dwarfs, an approach also applied to the Solar System's terrestrial planets (e.g., Clement et al. 2023). Alternatively, Wu et al. (2024a) argue that the observed period-ratio and eccentricity

distributions can be reproduced by starting from a uniform distribution of embryos and then allowing resonant kicks—gravitational scattering during brief resonant encounters—to dynamically rearrange the orbits into the observed configuration.

Recent observations provide mounting support for the broken-chain scenario. The right panel of Fig. 1.6 reveals that young planetary systems (age $\lesssim 100$ Myr) exhibit a high fraction (80–90%) of planet pairs near commensurate period ratios, whereas older systems show a much lower resonant fraction (roughly 10%). Moreover, Leleu et al. (2024) found that planets far from resonance tend to be more massive than those that remain in resonance. These trends are consistent with a picture in which planets initially migrate into resonant chains, but subsequently break resonance through violent dynamical scattering and merger events.

1.3.2 The Solar System

Compared to many observed exoplanetary systems, the planets of the Solar System present a somewhat similar configuration in terms of resonance: None of the eight planets is currently locked in mean motion resonances, similar to many compact, evolved exoplanetary systems. The study on the formation of the Solar System started earlier due to more observations than the exoplanet systems.

In the Nice model, the giant planets (Jupiter, Saturn, Uranus, Neptune, often with an additional ice giant) are initially assumed to form in a multi-resonant configuration (Tsiganis et al. 2005). Subsequent interactions with a residual planetesimal disk Griveaud et al. (2024), photoevaporative disk front (Liu et al. 2022), or star flybys (Kaib & Raymond 2025) destabilize the primordial resonances, leading to a period of orbital rearrangement and planet scattering that shapes the current architecture. This scenario provides a natural explanation for the current spacing and eccentricities of the outer planets, Kuiper belt distribution, and some other features in the outer Solar System.

The formation of the Solar System’s inner terrestrial planets started with a well-known puzzle: the small Mars problem. Classical in-situ accretion models consistently produce a Mars that is too massive and fail to replicate the stark mass contrast between Earth and Mars. Then a breakthrough came with the idea that the terrestrial planets accreted from a narrow annulus of planetesimals situated roughly between 0.7 and 1.0 au, rather than from a broad disk extending to the present orbit of Mars. This confined initial distribution, when combined with perturbations from the outer giant planets, naturally truncates the outer disk. It leaves insufficient material to form a large Mars and successfully reproduces the observed planetary masses and orbital spacing (Walsh et al. 2011).

More recent work has further refined this picture by introducing a two-ring model of terrestrial planet formation. This approach is motivated by the desire to place planet formation within a more physically realistic, earlier phase of the solar nebula. In the two-ring model, planetesimals form concurrently in distinct inner and outer rings, separated by a gap likely created by silicate sublimation or other processes in the young, gas-rich disk. This structure provides a more natural initial condition consistent with astrophysical disk models and allows terrestrial accretion to begin earlier, during the nebular phase. Many of the protoplanets are also formed in resonance chains. As demonstrated by Nesvorný et al. (2025), this framework can additionally match the terrestrial planet oxidation states compared to single-ring models.

1.4 This Thesis

To understand the complex nature of planet formation, one obvious thing to do is to study planet architectures, which preserve imprints of planet evolution histories. The work presented in this dissertation focuses on unraveling the dynamical history of planet systems in resonance and potential broken resonance chains, with N-body simulations, statistics, and planet formation modeling. This Thesis covers the three exoplanet system categories in Fig. 1.7: perfect resonance chains, special resonance chains and broken resonance chains.

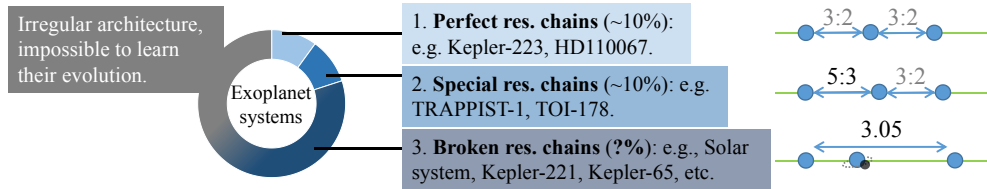


Figure 1.7. Classifying planet system architectures by how pristine their resonance chains are.

When, where, and how many exoplanets end up in orbital resonances?

Protoplanetary disks are the birthplaces of planets. As protoplanets exchange angular momentum with the surrounding disk, they migrate. Migration can capture two planets in a stable mean motion resonance, as observed in systems such as PDS70 (2:1 resonance Bae et al. 2019) and TRAPPIST-1 (resonance chain Luger et al. 2017). However, too rapidly migrating planets result in resonance crossing instead of trapping. Here, I have derived the critical migration rate delineating the transition between resonance trapping and crossing, providing a tool for the community to diagnose the birth disk mass of perfect resonance chain planets. Because fast migration typically entails the existence of a massive disk, I also calculated that near-resonant exoplanets were formed in disks with masses comparable to the Minimum Mass Solar Nebula. Around the same time that I archived my paper, Batygin & Petit (2023a) independently derived an equivalent resonance-trapping criterion using a different approach.

The dynamics of special chain systems and their formation: TRAPPIST-1

Higher-order resonance chains allow us to constrain planet formation timescales. For example, in the TRAPPIST-1 system, the high-order 8:5 and 5:3 resonances of its inner three planets are near-impossible to replicate if the planets stayed within the disk (Teyssandier et al. 2022; Burn et al. 2021). These resonances can only be obtained when the inner planets migrated into a gas-free magnetospheric cavity, where disk torques expand their original 3:2 resonances to the observed higher-order resonances. In addition, the outer planets d, e, and f can neither form too fast nor too slow, otherwise the planets would result in a configuration incompatible with observation. In this way, I offered an approach to constrain the formation timescales of exoplanets from their present-day architectures. Recent magnetohydrodynamic simulations (Romanova et al. 2025) confirmed our proposed cavity migration mechanism. Our proposed pathway for TRAPPIST-1 is also applicable to other resonance chain systems, e.g., TOI-178, and HD158259.

The dynamics of broken chain systems and their formation: the Solar System

While many systems exhibit resonances, others, including our Solar System, do not. Various mechanisms, such as disk dispersal (Izidoro et al. 2021), stellar flybys (Maas et al. 2025), and planetesimal collisions (Li et al. 2024; Yi et al. 2025a), can disrupt primordial resonances. In

the Solar System, the giant planet instability (Morbidelli et al. 2005) perturbs inner terrestrial planets through secular interactions (Kaib & Chambers 2016). Here, the present-day dynamical structure of the Solar terrestrial planets naturally emerges when these planets started in a resonance chain that was destabilized during the giant planet instability, resulting in the Moon-forming impact. Our findings support the view that the Solar terrestrial planets formed early, in a gas-rich disk, analogous to exoplanet systems. It also offers a new testable way for multi-planet systems to break primordial resonances, as most planet systems exhibit.

Suppression of giant planet formation in star cluster environments

Observation already revealed that the birth environment of stars significantly impacts the planet-forming disks. The examples are the observed Proplyds in the Orion Nebula (Berné et al. 2024) as well as numerical simulations (Wilhelm et al. 2023). This study introduces a simplified planet population synthesis code that simulates planet formation in the proplyds in an Orion-like cluster, incorporating factors such as pebble accretion and the effects of nearby stellar radiation on protoplanetary disks. The simulations show that clustered environments hinder the formation of giant planets, especially around low-mass stars. Neptune-sized planets on wide orbits are formed instead. The reason is that the short disk life time halt both planet gas accretion and migration. The large population of Neptune-sized planets at Jupiter-like orbits is consistent with recent Microlensing discoveries (Zang et al. 2025).

Signature of closely-spaced pebble-accreting protoplanets in ALMA disks

While exoplanets on wide orbits are relatively common, not so many protoplanets have been found. It has been shown that the occurrence rate of substructures in disks is comparable to the occurrence rate of exoplanets (van der Marel & Mulders 2021). This study propose many of the protoplanets are too small to be detected. The transition disks are categorized into two distinct groups based on their properties and the types of planets they may host. In Group A, massive gas giants create deep gaps in the gas disk, while in Group B, multiple smaller Neptunian-like planets contribute to the formation of inner dust cavities without creating substantial gas gaps. The characteristics of the dust rings formed in these disks—such as sharp inner edges—can provide critical insights into the underlying planet formation processes. The observational implications of these findings suggest that high-resolution imaging techniques, particularly with the Atacama Large Millimeter/submillimeter Array (ALMA), could further validate these models and enhance our understanding of planet formation in various disk environments.

1.5 Outlook: confirm and characterize broken chains

This thesis has shown that compact systems without strong external perturbations can preserve their primordial resonant chains over \sim Gyr timescales (e.g., Tamayo et al. 2017). In contrast, the breakage of such a chain is driven by post-formation perturbations, resulting in a Solar terrestrial planet-like configuration (see Fig. 1.8). Both intact and broken resonant chains encode valuable information about a system’s migration and evolution history. However, while intact chains are relatively straightforward to identify through period commensurabilities, broken chains are far more observationally elusive. Their identification represents a significant challenge, but also a compelling opportunity, in exoplanet science. The detection and characterization of such systems would address many fundamental questions in planet formation theories. To advance this search, future work should pursue two complementary lines of evidence: Orbital architecture and planetary composition.

Broken resonance chains in exoplanet systems

Disrupted resonance chains are much harder to identify than intact ones, but near-integer period ratios can act as dynamical relics of primordial resonances (Cambioni et al. 2025). Analogous to the 3.05 period ratio between Venus and Mars, several *Kepler* systems show similar signatures. For example, in Kepler-48 the inner pair lies near a 2:1 commensurability, while an outer giant planet may have disrupted the original chain. In Kepler-65, the b-d pair lies close to a 15:4 ratio, consistent with the remnant of an original 2:1–3:2–4:3 chain in which planet c plausibly formed via a merger. The Kepler-221 system exhibits a comparable architecture (Yi et al. 2025a).

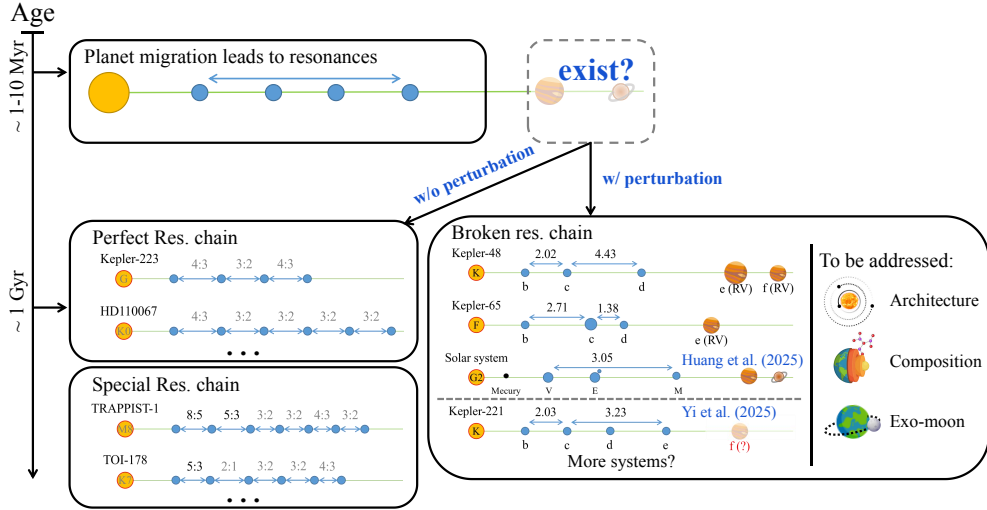


Figure 1.8. Sketch of the dichotomy evolution of a primordial resonance chain. If there are no external perturbations, the resonance chains are preserved (left). The resonances of each adjacent planet pair are labeled. If there are perturbations, the resonance chains are destabilized (right). The relevant period ratios are labeled.

A natural extension of my PhD work is to conduct a systematic survey of the ~ 330 known multi-planet systems, using analytical criteria and N-body simulations to determine whether their present architectures can arise from initially resonant chains that were later destabilized. This will generalize the framework developed in Yi et al. (2025a) and Huang et al. (2025) to a population-level test. For systems that show evidence of disruption but lack detected outer giants, dynamical modeling can be used to infer whether unseen companions are required, a prediction that can be tested with forthcoming Gaia DR4 astrometry.

Compositional signatures of chain disruption

Chain destabilization is expected to trigger close encounters and giant impacts, leaving observable imprints on planetary radii, densities, and atmospheres. In Kepler-65, for instance, planet c ($2.5 R_{\oplus}$) is substantially larger than its neighbors b and d ($\sim 1.5 R_{\oplus}$), consistent with a merger origin and possible post-impact atmosphere loss (Biersteker & Schlichting 2021). More generally, planets that experienced giant impacts should be denser and more depleted in primordial volatiles or even host moons, like the Earth-Moon system.

By combining N-body simulations with models of impact outcomes based on smoothed-particle hydrodynamics (Emsenhuber et al. 2024; Dou et al. 2024), I will identify the most likely post-impact planets in broken-chain systems. These predictions can be tested through

precise mass measurements from radial-velocity surveys and atmospheric characterization with JWST, allowing the broken-chain scenario to be probed from both dynamical and compositional perspectives.

Looking further ahead, a powerful suite of next-generation facilities will enable the systematic characterization of smaller exoplanets. This includes ground-based giants like the Extremely Large Telescope (ELT), Giant Magellan Telescope (GMT), and Thirty Meter Telescope (TMT), alongside space-based observatories such as the Habitable Worlds Observatory, PLATO, ARIEL, and the Roman Space Telescope. Together, they will probe atmospheric biosignatures and habitability, bringing us closer to answering the ultimate questions of how common Solar System-like architectures are and how we came to be here.

